

UC Berkeley

UC Berkeley Previously Published Works

Title

Modeling the Time-Dependent Concentrations of Primary and Secondary Reaction Products of Ozone with Squalene in a University Classroom

Permalink

<https://escholarship.org/uc/item/6n63j3qd>

Journal

Environmental Science and Technology, 53(14)

ISSN

0013-936X

Authors

Xiong, Jianyin

He, Zhangcan

Tang, Xiaochen

et al.

Publication Date

2019-07-16

DOI

10.1021/acs.est.9b02302

Supplemental Material

<https://escholarship.org/uc/item/6n63j3qd#supplemental>

Copyright Information

This work is made available under the terms of a Creative Commons Attribution-NonCommercial License, available at <https://creativecommons.org/licenses/by-nc/4.0/>

Peer reviewed

1 **Modelling the time-dependent concentrations of primary and**
2 **secondary reaction products of ozone with squalene in a**
3 **university classroom**

4 Jianyin Xiong^{1,2,*}, Zhangcan He¹, Xiaochen Tang³, Pawel K. Misztal^{2,4}, Allen H.
5 Goldstein^{2,5}

6

7 ¹ School of Mechanical Engineering, Beijing Institute of Technology, Beijing 100081,
8 China

9 ² Department of Environmental Science, Policy and Management, University of
10 California, Berkeley, California 94720, United States

11 ³ Indoor Environment Group, Energy Technologies Area, Lawrence Berkeley National
12 Laboratory, Berkeley, CA 94720, United States

13 ⁴ Centre for Ecology & Hydrology, Edinburgh, Midlothian, EH26 0QB, UK

14 ⁵ Department of Civil and Environmental Engineering, University of California,
15 Berkeley, CA, United States

16

17 *Corresponding author. Tel.: +86 10 68914304; Fax: +86 10 68412865; E-mail address:

18 xiongjy@bit.edu.cn

19 **Abstract**

20 Volatile organic chemicals are produced from reactions of ozone with squalene in
21 human skin oil. Both primary and secondary reaction products, i.e., 6-methyl-5-hepten-
22 2-one (6-MHO) and 4-oxopentanal (4-OPA), have been reported in indoor occupied
23 spaces. However, the abundance of these products indoors is a function of many
24 variables including the amount of ozone and occupants present as well as indoor
25 removal processes. In this study, we develop a time-dependent kinetic model describing
26 the behavior of ozone/squalene reaction products indoors, including the reaction
27 process and physical adsorption process of products on indoor surfaces. The key
28 parameters in the model were obtained by fitting time-resolved concentrations of 6-
29 MHO, 4-OPA, and ozone in a university classroom on one day with multiple class
30 sessions. The model predictions were subsequently tested against observations from
31 four additional measurement days in the same classroom. Model predictions and
32 experimental data agreed well ($R^2=0.87-0.92$) for all test days including ~7 class
33 sessions covering a range of occupants (10-70) and ozone concentrations (0.09-32 ppb),
34 demonstrating the effectiveness of the model. Accounting for surface uptake of 6-MHO
35 and 4-OPA significantly improved model predictions ($R^2=0.52-0.76$ without surface
36 uptake), reflecting the importance of including surface interactions to quantitatively
37 represent product behavior in indoor environments.

38

39 **Introduction**

40 Ozone is typically the dominant oxidant in indoor air for chemicals containing
41 unsaturated carbon bonds, and thereby plays an important role in indoor air chemistry.¹
42 Indoor ozone generally originates from ventilation with outdoor air, and in some
43 environments could have additional sources such as ozonolysis air purifiers,
44 photocopiers or printers.²⁻⁴ Early studies on indoor ozone were mainly confined to
45 interactions with cleaning products and building materials,⁵⁻¹⁰ while just a few studies
46 referred to the direct interaction of ozone with humans. Later research discovered that
47 in highly occupied indoor spaces the main loss process for ozone is typically reaction
48 with the unsaturated carbon-carbon double bonds in human skin oil. For example,
49 human occupants were shown to be the most important sinks for ozone in a simulated
50 aircraft cabin environment, accounting for ~60% of ozone removal.¹¹ Ozone has also
51 been shown to react with human skin oil remaining on hair and worn clothing.¹²⁻¹⁴

52 Human skin oil is composed of fatty acids, glycerides, wax esters and squalene.
53 Squalene, a triterpenoid hydrocarbon containing six unsaturated carbon-carbon double
54 bonds, is the most abundant ozone-reactive constituent in skin oil, and is ubiquitous in
55 occupied indoor environments.¹⁵ Squalene ozonolysis products include acetone, 6-
56 methyl-5-hepten-2-one (6-MHO), geranyl acetone (Ga), 4,9,13,17-tetramethyl-
57 octadeca-4,8,12,16-tetraeneal (TOT), 4,8,13,17,21-tetramethyl-octadeca-4,8,12,16,20-
58 pentaene-al (TOP), and 5,9,13-trimethyl-tetradeca-4,8,12-triene-al (TTT). Primary
59 products with remaining unsaturated carbon-carbon double bonds can react with ozone
60 again generating secondary products,¹⁶ such as 4-oxopentanal (4-OPA), which is

61 recognized as an asthma trigger and sensitizer, and has been shown to induce irritation
62 and allergic response.¹⁷⁻²⁰ The ozonolysis of fatty acids also leads to formation of
63 various aldehydes (i.e., decanal, nonanal, hexanal, octanal, undecanal), and the yields
64 of the last three products are generally lower.²¹ The reaction of ozone with human skin
65 oil has also been shown to result in the indoor formation of secondary organic
66 aerosols.^{14,22,23}

67 The heterogeneous reaction rate constants of ozone with pure squalene films under
68 different conditions have been reported from laboratory studies.^{21,24-26} Wells et al.²⁴
69 applied a pseudo first-order model to analyze the kinetics of ozone/squalene reaction
70 by coupling a second-order reaction with surface ozone. The first-order rate constant
71 was reported to be $1.58 \times 10^{-3} \text{ s}^{-1}$ with 50 ppb ozone. The kinetics were further examined
72 by Petrick and Dubowski,²¹ and the first-order rate constant was obtained as 1.22×10^{-5}
73 s^{-1} with 50 ppb ozone, much lower than that found by Wells et al. Fu et al.²⁵ analyzed
74 the reaction probability of squalene upon exposure to ozone, and acquired first-order
75 rate constants of $(2.5 \pm 0.3) \times 10^{-4} \text{ s}^{-1}$ and $(6.3 \pm 0.6) \times 10^{-3} \text{ s}^{-1}$ for C=C band and C=O
76 band with 250 ppb ozone. Zhou et al.²⁶ investigated squalene film changes when
77 exposing to ozone and the reactive uptake coefficients were determined to be (1.3 ± 0.1)
78 $\times 10^{-3} \text{ s}^{-1}$ and $(6.0 \pm 0.4) \times 10^{-4} \text{ s}^{-1}$ for ozone mix ratio of 50 ppb and 25 ppb. These
79 studies represent a range of second-order rate constants of $(0.02-3.15) \times 10^{-5} \text{ s}^{-1} \text{ ppb}^{-1}$
80 for primary products of ozone/squalene reactions. A few studies also investigated the
81 rate constants for secondary products.^{27,28} The large discrepancy in the rate constants of
82 ozone with pure squalene film in laboratory among different studies implies the reaction

83 dynamics are not fully understood. Wisthaler and Weschler²⁹ observed that the
84 predicted secondary product (4-OPA) concentration based on rate constants determined
85 from lab tests was much lower than the measured data in a simulated office. Tang et
86 al.³⁰ reported observations of these products and their dynamic behavior in a classroom
87 regularly occupied by students over a period of several weeks, providing the dataset
88 used here for further study of the processes determining their abundance in indoor air.

89 A few model investigations have been reported simulating the dynamic
90 interactions of airborne chemicals with human skin. These models are generally limited
91 to physical transport processes,^{31,32} while one model is specifically simulating chemical
92 reactions of ozone with squalene. Lakey et al.¹⁶ extended a kinetic multilayer model
93 used for predicting the oxidation of oleic acid particles to skin oil, and developed a
94 kinetic multilayer model of surface and bulk chemistry of the skin (KM-SUB-Skin) to
95 simulate the emission of squalene ozonolysis products from people exposed to ozone.
96 They applied this model to simulate ozone, 6-MHO, and 4-OPA for comparison with
97 three sets of data collected in simulated office and small enclosure. The model includes
98 tens of parameters that must be determined, thus presenting a barrier to its wide use in
99 engineering applications. In addition, the model ignores adsorption and desorption
100 processes of products onto indoor surfaces, which should cause prediction
101 discrepancies in real indoor environments since surface interactions are important for
102 these types of chemicals and must influence the indoor composition as well as chemical
103 dynamics.³³

104 The objectives of the present study are to: (1) develop a novel kinetic model that

105 predicts the products of chemical reactions between ozone and squalene including their
106 interaction with indoor surfaces; (2) analyze data from a previously reported
107 measurement campaign in a university classroom³⁰ to validate the model and examine
108 the behavior of reaction products in this typical indoor setting with varying occupant
109 density and ozone concentrations.

110

111 **Methods**

112 Heterogeneous oxidation of squalene by ozone produces aldehydes, ketones and
113 some bicarbonyl compounds.²¹ Two of the most abundant primary and secondary
114 products are 6-MHO and 4-OPA,²⁹ which can irritate the digestive tract, respiratory
115 tract, skin and eyes (6-MHO), and induce allergic response (4-OPA),^{17-20,34} and these
116 are selected as typical main products for our modeling analysis. Formation of 6-MHO
117 occurs as a product of the primary reaction between ozone and squalene, while
118 formation of 4-OPA is a product of the secondary reactions of ozone with 6-MHO, as
119 well as ozone with geranyl acetone.^{21,29} The detailed chemical reactions are given by
120 equations (S1)-(S3) in Section S1 of the Supporting Information (SI). The time-
121 dependent ozone concentration in indoor air (classroom for the present study) can be
122 characterized by the following equation:

$$V \frac{dC_{O_3}(t)}{dt} = Q[C_{in,O_3}(t) - C_{O_3}(t)] - v_{d,h} A_h C_{O_3}(t) - v_{d,r} A_r C_{O_3}(t) \quad (1)$$

123 where C_{O_3} is the ozone concentration in the classroom air, ppb; C_{in,O_3} is the ozone
124 concentration introduced into the classroom in the supply air, ppb; V is the volume of
125 the classroom, m^3 ; A_h and A_r are the surface areas of the human bodies and room

126 surfaces, respectively, m^2 ; Q is the ventilation rate, $m^3 s^{-1}$; $v_{d,h}$ and $v_{d,r}$ are the deposition
127 velocities of ozone at the human skin surfaces and indoor surfaces, respectively, $m s^{-1}$.

128 Prior modeling studies generally focused on ozone/squalene reactions with
129 constant inlet ozone concentrations,^{21,24-29} while the present study examines the
130 reactions with naturally varying ozone concentrations in the ventilation supply air
131 which comes from outdoors. The formation rate of 6-MHO and 4-OPA are described in
132 SI Section S2. In real indoor environments, the chemicals (e.g., 6-MHO, 4-OPA) will
133 adsorb/desorb onto the wall surfaces. This surface partitioning for squalene oxidation
134 products was not considered in previous indoor modelling.^{16,35} Previous studies
135 generally focused on chamber experiments or indoor spaces with high air change rates
136 such as an aircraft cabin at $25-30 h^{-1}$,^{16,36} and assumed wall effects were negligible. Our
137 model explicitly account for wall effects to determine their significance for indoor
138 environments such as the classroom we are studying which has an air change rate of 5
139 h^{-1} .³⁷ For surface partitioning, we assume that a convective boundary layer exists along
140 the wall surface, and the wall uptake/release rate can be represented as:

$$E(t) = h_{m,s}(C_a - C_s) = K_s \frac{dC_s}{dt} \quad (2)$$

141 where C_s is the surface concentration of chemicals, ppb; K_s is the surface/air partition
142 coefficient, m (for 6-MHO and 4-OPA, the partition coefficients are expressed as K_{6M}
143 and K_{4O} , respectively); $h_{m,s}$ is the convective mass transfer coefficient across the wall
144 surface, $m s^{-1}$.

145 The mass balance equation for 6-MHO and 4-OPA can then be represented as:

$$V \frac{dC_{6M}(t)}{dt} = A_h \cdot k_{6M} \cdot C_{O_3} + Q \cdot [C_{in,6M}(t) - C_{6M}(t)] - V \cdot k_{4O} \cdot C_{O_3} \cdot C_{6M}(t) + V \cdot k_{Ga} \cdot C_{O_3} \cdot C_{Ga}(t) - A_r \cdot E_{6M}(t) \quad (3)$$

$$V \frac{dC_{4O}(t)}{dt} = V \cdot k_{4O} \cdot C_{O_3} \cdot C_{6M}(t) + V \cdot k_{Ga} \cdot C_{O_3} \cdot C_{Ga}(t) + Q \cdot [C_{in,4O}(t) - C_{4O}(t)] - A_r \cdot E_{4O}(t) \quad (4)$$

146 where C_{6M} is the concentration of 6-MHO in the classroom air, ppb; C_{4O} is the
 147 concentration of 4-OPA in the classroom air, ppb; C_{Ga} is the concentration of geranyl
 148 acetone in the classroom air, ppb; $C_{in,6M}$ is the 6-MHO concentration in the supply air,
 149 ppb; $C_{in,4O}$ is the 4-OPA concentration in the supply air, ppb; k_{6M} is the pseudo-first-
 150 order rate constant of 6-MHO, $m\ s^{-1}$; k_{4O} is the second-order rate constant of 4-OPA, s^{-1}
 151 ppb^{-1} ; k_{Ga} is the second-order rate constant of geranyl acetone, $s^{-1}\ ppb^{-1}$.

152 The concentrations of ozone, 6-MHO and 4-OPA in indoor environments can be
 153 characterized by equations (1), (3) and (4). Eight key parameters should be pre-
 154 determined to calculate three pollutant concentrations (C_{O_3} , C_{4O} , C_{6M}), i.e., $v_{d,h}$, $v_{d,r}$, k_{6M} ,
 155 k_{4O} , k_{Ga} , K_{6M} , K_{4O} , C_{Ga} . Previous study assumes that 6-MHO and geranyl acetone have
 156 equal production rates from the reactions of ozone with squalene, and the second-order
 157 rate constant of geranyl acetone (k_{Ga}) is half of that for 6-MHO.¹⁶ In order to determine
 158 the remaining key parameters, experiments must be performed to measure the time-
 159 resolved concentrations of ozone, 6-MHO and 4-OPA in the indoor environment,
 160 including the amount coming in through ventilation. Then the remaining parameters
 161 can be extracted by fitting the kinetic model with experimental data through nonlinear
 162 curve regression. In the present study, to ensure the accuracy of the obtained parameters,
 163 data collected on one test day were generally used to determine the key parameters in

164 the kinetic model, and data from other four test days were then used to assess model
165 performance by comparison with observations.

166

167 **Experimental section**

168 Measurements were carried out over a period of five days (Nov 4, Nov 5, Nov 6,
169 Nov 12, Nov 13, 2014) in a typically occupied classroom located at the University of
170 California, Berkeley. The experimental setup, and results of concentrations and fluxes
171 from outdoor, indoor, and occupant sources have been previously reported,^{30,38} thus
172 only a brief description is provided here. The volume of the classroom was 670 m³, and
173 ambient ozone was introduced from outdoors directly through the single-pass
174 ventilation system (the outdoor ozone concentration changed over time). The number
175 of occupants (students) in the classroom was recorded manually, and fluctuated from
176 10-70 during different class sessions, as seen in SI Table S1. The ratio of male to female
177 was 66%:34% during the test, and the use of personal care products and its influence
178 on indoor air composition was analyzed in a prior study.³² Measurements were also
179 made during unoccupied conditions when classes were not in session. During the
180 experiments (field campaign), a proton-transfer-reaction time-of-flight mass
181 spectrometer (PTR-TOF-MS) (IONICON Analytik GmbH) was used to measure the
182 concentrations of 6-MHO and 4-OPA as well as other volatile organic compounds in
183 the classroom and supply air (switching at 5-minute intervals), daily from 8:10 am to
184 20:45 pm. This instrument uses H₃O⁺ as the primary reagent, and can scan the mass
185 spectrum for mass-to-charge ratio (*m/z*) of 30-500. PTR-TOF-MS enables fast response

186 time measurements (full mass spectrum in seconds or minutes), has high sensitivity
187 (tens of parts per trillion or ppt in a second), and high mass resolution.^{30,39} After 18:00
188 pm, the classroom was always empty but the ventilation remained on for several more
189 hours. The time-dependent ozone concentrations in the classroom and supply air were
190 continuously monitored with an ozone analyzer (Thermo Scientific 49i) through the
191 same sampling lines.

192 The walls and ceiling in the classroom were covered with latex paint, and the floor
193 was made of hard tile and cleaned periodically outside of normal class times. The total
194 surface areas of walls, floor, and ceiling in the classroom was estimated to be 534 m²
195 based on the physical dimensions (length, width, height). The surface area of tables and
196 chairs exposed to ambient air in the classroom was estimated to be 65 m² in total. The
197 mechanical single-pass ventilation system provides an air change rate (N) of 5 ± 0.5 h⁻¹
198 ^{1, 37} using outdoor air for the supply so ozone concentration of air entering the classroom
199 varies with outdoor air concentrations. The surface area of each human body is assumed
200 to be 1.7 m².⁴⁰ The convective mass transfer coefficient along the wall surface is about
201 0.002 m s⁻¹, calculated by empirical correlations, consistent with the commonly
202 reported range (0.0007-0.004 m s⁻¹).⁴¹⁻⁴³ The parameters used for modeling are
203 summarized in SI Table S2.

204

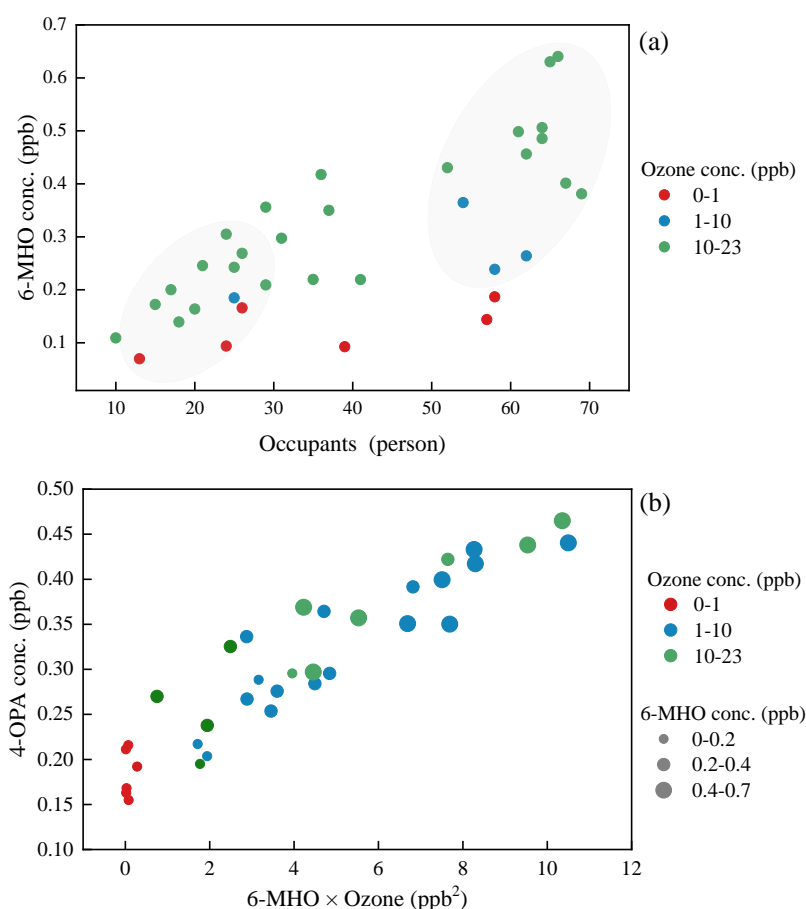
205 **Results and discussion**

206 **Observations and relationships among occupant number, ozone level and** 207 **oxidation products**

208 The measured data of five test days in the classroom covers a series of squalene
209 oxidation products concentrations and some important influencing factors (ozone,
210 occupancy, 6-MHO, and 4-OPA), thus it makes sense to probe their relationships from
211 this dataset. We averaged the measured data for each classroom session and took the
212 processed data for analysis. The processed ozone concentration covers a wide range (0-
213 23 ppb). For the convenience of visualization, the ozone concentration is divided into
214 three intervals (0-1 ppb, 1-10 ppb and 10-23 ppb for each interval). After data transform,
215 we bin all the data according to the ranges of ozone concentration, and then plot bins
216 (6-MHO vs occupancy, 4-OPA vs product of 6-MHO and ozone bins) into Figure 1. In
217 the figure, ozone concentrations are marked by different colors (red, blue and green).
218 To more clearly show the relevance of 4-OPA with 6-MHO and ozone, further data
219 transform is performed for Figure 1(b). We divide 6-MHO concentrations into three
220 intervals (0-0.2 ppb, 0.2-0.4 ppb and 0.4-0.7 ppb for each interval) and mark them in
221 the manner of the circle size (circle size from small to large indicates concentration
222 from low to high). With above processing, we can more clearly examine the impact of
223 occupants and ozone levels on the squalene oxidation products.

224 As is shown in Figure 1(a), two clusters are differentiated by the number of
225 occupants and ranges of ozone concentration to determine if certain behaviors exist. In
226 the left cluster, the number of occupants is small (10-30 persons) and the average 6-
227 MHO concentration is low (0.07-0.30 ppb); while in the right cluster, the number of
228 occupants is large (50-70), with high average 6-MHO concentration (0.24-0.64 ppb). It
229 is clear that occupants do influence the abundance of 6-MHO, with an increasing

230 tendency. The observed behavior is consistent with our fundamental understanding, i.e.,
 231 low 6-MHO at low ozone and occupancy levels, high 6-MHO at high ozone and
 232 occupancy levels. Figure 1(b) indicates that the concentration of 4-OPA is
 233 approximately in a linear relationship with the product of concentrations of 6-MHO and
 234 ozone. When the concentrations of ozone and 6-MHO are low (smallest red circle), 4-
 235 OPA concentration is at a low level. When the concentrations of ozone and 6-MHO are
 236 high (largest blue and green circles), 4-OPA concentration is accordingly at a high level.
 237 It should be pointed out that, 4-OPA will continue to produce even if without occupants
 238 because the reactions between ozone with 6-MHO and geranyl acetone in gas phase are
 239 still in process.



240

241

242 **Figure 1.** Scatter plots of (a) 6-MHO versus number of occupants and (b) 4-OPA versus

243 the product of 6-MHO and ozone, for average data from each class session of five test
244 days (Ozone concentration bins are marked by different colors; 6-MHO concentrations
245 are marked in the manner of circle size).

246

247 **Determining ozone deposition velocity to room surfaces**

248 The measured classroom/supply ozone data during the unoccupied period from
249 18:10 pm to 20:45 pm on Nov 6, 2014 is used in equation (1) to determine the ozone
250 deposition velocity to room surfaces ($v_{d,r}$). To simplify the calculation, we assume all
251 the indoor surfaces have the same deposition velocity and the objective function is then
252 a 2-norm solution of the difference between the predicted value and measured value.
253 The optimal parameter value is obtained by minimizing the objective function. During
254 the global optimization process, a pattern search algorithm is applied. The determined
255 ozone deposition velocity to room surfaces is 0.03 cm s^{-1} , in agreement with typical
256 values published for common indoor materials ($0.02\text{-}0.058 \text{ cm s}^{-1}$, listed in SI Table S3).
257 Model predictions of ozone concentration in the classroom are compared with measured
258 data in some other days as shown in SI Figure S1. The good agreement suggests the
259 reliability of the determined deposition velocity.

260

261 **Determining ozone deposition to human surfaces**

262 The measured ozone data with occupants in the classroom on the same day (Nov
263 6) is then used for determining ozone deposition velocity to human surfaces ($v_{d,h}$).
264 Classroom occupancy varied from 15 to 58 during this period, and human surface area

265 was scaled accordingly in a time-dependent manner. While ozone removal to human
266 surfaces is fairly sensitive to the near surface air movement,¹³ and ozone deposition
267 velocity can vary between different individuals, the range of occupancy in the
268 classroom during this day provides a good opportunity to determine an average value
269 relevant to highly occupied spaces. The fitted value as well as model prediction for
270 classroom ozone are listed in Table 1 and Figure 2(a). The 9-h average deposition
271 velocity for ozone removal by occupants for the classroom of 0.25 cm s^{-1} is in the range
272 of literature values (0.20 to 0.62 cm s^{-1} , SI Table S3). It is clear that ozone deposition
273 velocity to human skin surfaces is nearly one order of magnitude larger than that to
274 indoor surface, thus when human surface area approaches one tenth of the room surface
275 area, these removal processes become approximately equivalent.

276 It is also instructive to compare the relative contribution of ozone deposition to
277 occupant and room surfaces with removal to human breathing and gas-phase reaction.
278 The rate constants of typical indoor VOCs (excluding squalene ozonolysis products)
279 reacting with ozone are in the range of 10^{-13} - $10^{-7} \text{ s}^{-1} \text{ ppb}^{-1}$, which is much lower than
280 that of ozone/squalene reaction probability (see the “Introduction” section).⁴⁴ It should
281 be noted that the chemical loss of ozone due to gas-phase reaction could potentially be
282 competitive in transient cases of high levels (10-100 ppb) of typical indoor VOCs (e.g.,
283 monoterpenes that react with ozone) during fresh emission episodes. Nevertheless, the
284 influence from monoterpene chemistry did not seem apparent in the classroom based
285 on the low level of monoterpene oxidation products (<5 ppb) which makes sense given
286 the high air change rates (5 h^{-1}). Undoubtedly, peeling citrus fruit, and using detergents,

287 can release a series of monoterpenes, and the concentration of some common
288 monoterpenes (such as limonene, terpene alcohol, α -pinene) can be high in some places.
289 For the present study, the 8-h average concentration of these reactive species was less
290 than 2 ppb in the classroom for Nov 13.³⁸ Morawska et al.⁴⁵ also measured the limonene
291 concentration in a classroom located in Brisbane and found that the 24-h average
292 mixing ratio of limonene was less than 2 ppb. Based on these data, we simplify the
293 model and ignore the gas-phase chemistry of ozone with monoterpenes for the cases
294 studied. The caveat should be kept in mind that the developed model is more applicable
295 for low-monoterpene circumstances.

296 For the convenience of calculation, the determined deposition velocities are
297 converted into ozone removal rates, and the number of occupants in the classroom is
298 set as 57 persons. The estimated first-order removal rates for occupant surfaces and
299 room surfaces are 1.3 h^{-1} and 0.97 h^{-1} , respectively. Ozone can be also removed by
300 respiration. By assuming the breathing rate of a sedentary adult is $0.52 \text{ m}^3 \text{ h}^{-1}$,^{11,46} and
301 that breathed ozone is completely removed in the body before the breath is exhaled, the
302 ozone removal by occupants breathing in the classroom is estimated to be 0.043 h^{-1} . SI
303 Figure S2 presents the relative contribution of various sinks to ozone removal in the
304 classroom. Among these sinks, occupants account for the largest relative contribution,
305 almost 60%. This ratio is similar to values reported in the literature (58% in a simulated
306 aircraft cabin).¹¹ Although the deposition velocity of ozone removal to indoor surfaces
307 is only one-tenth of that to human surfaces, considering that the total surfaces of the
308 classroom are about 600 m^2 , the relative contributions of both are comparable in this

309 classroom when occupant number reaches 40 persons. Because breathing accounts for
310 only 2% of the total removal, and gas-phase ozone removal is negligible according to
311 the above analysis, it is reasonable to model without considering these two ozone
312 removal effects.

313

314 **Determination of key parameters in the kinetic model for 6-MHO and 4-OPA**

315 A similar method is used to determine the remaining key parameters by fitting
316 model (equations (3) and (4)) with the occupied experimental data on Nov 6. The
317 determined key parameters as well as model predictions are summarized in Table 1 and
318 Figure 2(b), (c). The pseudo first-order rate constant of ozone with squalene in the
319 classroom is determined to be $2.5 \times 10^{-4} \text{ m s}^{-1}$, which is calculated by assuming that the
320 squalene concentration adjacent to human skin surfaces is constant. This assumption is
321 reasonable since squalene is naturally occurring and continuously produced by the
322 human body. The first-order rate constant can be converted into the second-order rate
323 constant. The surface coverage of squalene in the skin calculated ranges from 1.2×10^{13}
324 molecules cm^{-2} to 1.2×10^{14} molecules cm^{-2} .²⁴ Thus, by dividing the average surface
325 coverage (6×10^{13} molecules cm^{-2}), the second-order rate constant is determined to be
326 $3.09 \times 10^{-5} \text{ s}^{-1} \text{ ppb}^{-1}$, which is within the range of prior studies (see the “Introduction”
327 section). Actually, the formation rate of 6-MHO will vary for different parts of the body.
328 Experiments performed on different parts of the human body indicated that the 6-MHO
329 mixing ratio adjacent to the human forehead was nearly 1.4-fold larger than that next
330 to the cheek and forearm.²⁹ The reason is that more skin oil exists on the forehead

331 surface compared with other parts of human body. Generally, the pseudo first-order rate
332 constant of ozone with squalene can vary over the skin surface, depending on the
333 reaction probability of the occupant surface, as shown by computational fluid dynamics
334 (CFD) simulations.⁴⁷

335 The reaction rate constant of ozone with 6-MHO is measured to be $3.8 \times 10^{-5} \text{ s}^{-1}$
336 ppb^{-1} ($1.5 \times 10^{-15} \text{ cm}^3 \text{ molecule}^{-1} \text{ s}^{-1}$ after unit conversion), which is higher than
337 experiments conducted by Grosjean et al. and Leonardo et al. ($3.94 \pm 0.4 \times 10^{-16} \text{ cm}^3$
338 $\text{molecule}^{-1} \text{ s}^{-1}$ and $5.9 \times 10^{-16} \text{ cm}^3 \text{ molecule}^{-1} \text{ s}^{-1}$, respectively).^{27,28} The above two cases
339 are all conducted without human presence. Wisthaler and Weschler²⁹ used the gas-phase
340 reaction rate constant ($4.03 \times 10^{-16} \text{ cm}^3 \text{ molecule}^{-1} \text{ s}^{-1}$) to estimate the 4-OPA
341 concentration in an office occupied by occupants, and found that the calculated
342 concentration was much lower than the measured data (<5%), meaning the rate constant
343 should be higher when occupant is involved. Therefore, the difference of the reaction
344 rate constant in different studies can be ascribed to the effect of occupants to a large
345 extent. That is to say, part of the product (i.e., 4-OPA) measured in the gas phase in the
346 classroom may originate from surface reaction, causing 4-OPA concentrations in the
347 classroom greater than that originating only from gas-phase reactions between ozone
348 with 6-MHO and geranyl acetone. In summary, 6-MHO is derived from surface reaction
349 adjacent to the surface of human skin, while 4-OPA can come from both surface and
350 gas-phase reactions. Further study is needed to determine surface reaction rate constant
351 in different parts of the human skin surface.

352

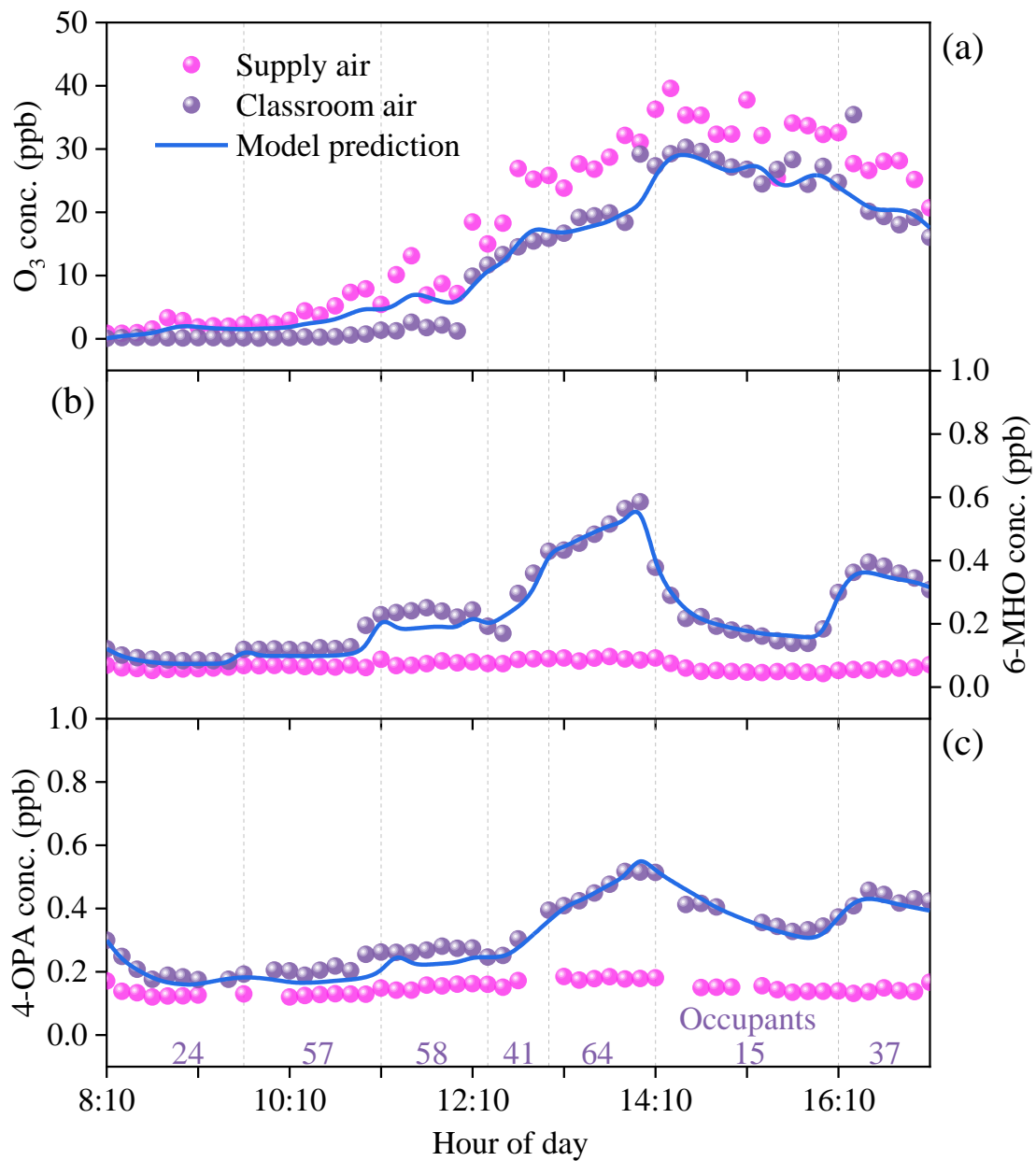
353 **Table 1.** Determined key parameters for ozone/squalene reactions

Parameters	Value
$v_{d,h}$	0.25 (cm s ⁻¹)
$v_{d,r}$	0.03 (cm s ⁻¹)
k_{4O}	3.8×10^{-5} (s ⁻¹ ppb ⁻¹)
k_{6M}	2.5×10^{-4} (m s ⁻¹)
K_s (6-MHO)	0.5 (m)
K_s (4-OPA)	0.9 (m)

354

355 Figure 2(a) shows that the outdoor ozone concentration was routinely higher than
 356 indoors, and the average ozone indoor-to-outdoor (I/O) concentration ratio was 0.7,
 357 which is within the expected range of 0.05 to 0.85 summarized in literature for different
 358 air change rates (0.05 for buildings tightly sealed and 0.85 for buildings with very high
 359 air change rates).⁴⁴ The temporal trend of indoor ozone concentration is similar to that
 360 of outdoors, reflecting that the air introduced into the classroom has variable amounts
 361 of ozone and classroom air volume is exchanged on a timescale of 12 min. Figure 2(b)
 362 and (c) show the fitted results for 6-MHO and 4-OPA. We can see that the
 363 concentrations of 6-MHO and 4-OPA outdoors are negligible in comparison to the
 364 classroom, and the trends of these two products are distinct from that of outdoors,
 365 reflecting the dominance of their sources due to ozone reactions with human skin oil.

366



367

368 **Figure 2.** Fitting results of modeled (a) ozone, (b) 6-MHO, and (c) 4-OPA compared
 369 with experimental observations from Nov 6, 2014, which were used to parameterize the
 370 model.

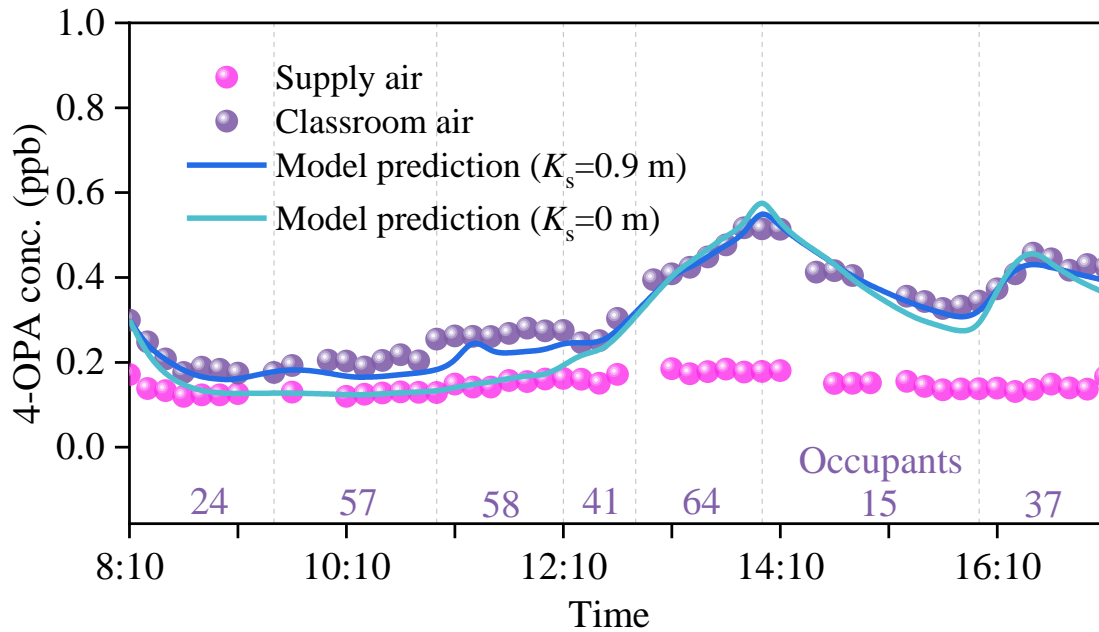
371

372 **Impact of surface partitioning**

373 Prior kinetic models focused on the reaction details of ozone with squalene, while
 374 the surface partitioning (adsorption/desorption) of products on the wall was not

375 considered. This effect should be included in typical indoor environments since the
376 surfaces of real buildings certainly will adsorb/desorb VOCs,⁴⁸ which will affect their
377 indoor concentrations. Figure 3 as well as Table 1 suggest that partitioning to surfaces
378 is significant both for 6-MHO and 4-OPA, because the model prediction departs from
379 the measured data when surface partitioning is excluded ($K_s=0$ m). The surface partition
380 coefficients for 6-MHO and 4-OPA are determined from the model fitting procedure to
381 be 0.5 m and 0.9 m, respectively. Predicted results without surface partitioning are
382 lower than the measured data in the morning because 4-OPA is adsorbed by wall surface
383 during the previous day and continues to desorb from surfaces in the morning when
384 production rates are low (low ozone). Later in the day around 14:00 pm when more
385 students are in the classroom and ozone is high, there is uptake by the classroom
386 surfaces, but during the subsequent class session when student occupancy drops to 15,
387 the 4-OPA begins coming off the walls enhancing the concentration in the classroom.
388 As far as we know, this is the first report that uses time-resolved measurements to
389 demonstrate and model the partition effects of 6-MHO and 4-OPA onto wall surface in
390 a real indoor environment.

391



392

393 **Figure 3.** Impact of surface partitioning on the modeled concentration of 4-OPA.

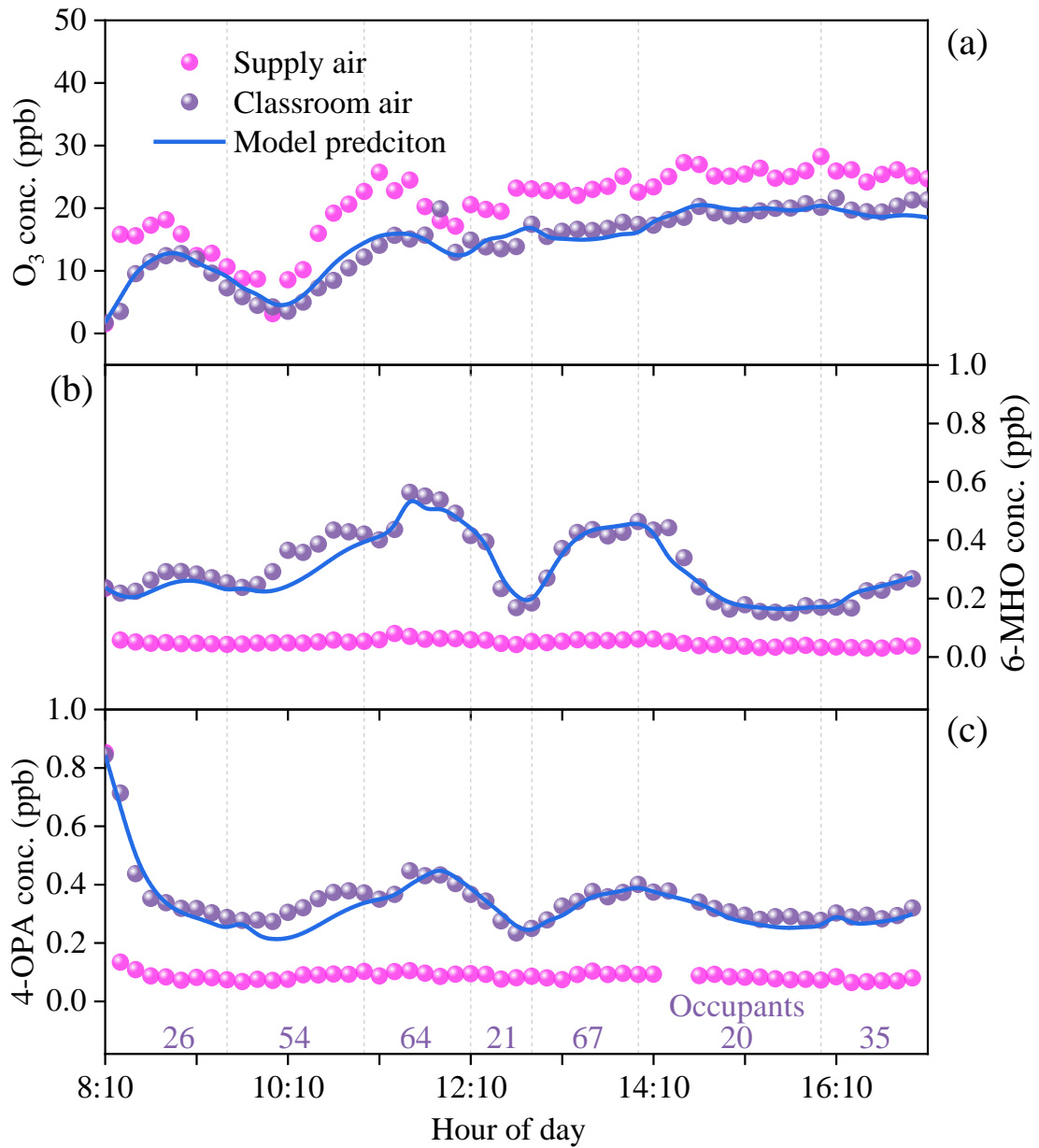
394

395 **Model validation**

396 In order to verify the efficacy of the kinetic model using the key parameters
 397 determined from data on Nov 6, 2014 (listed in Table 1), it is applied to predict the
 398 concentrations of ozone, 6-MHO and 4-OPA in four additional days of classroom
 399 observations (Nov 4, Nov 5, Nov 12, Nov 13). Measured and modeled results for Nov
 400 13 are presented in Figure 4 (comparisons for the other three test days are presented in
 401 SI Figures S3-S5). The number of occupants during this comparison day varied from
 402 20 to 67, and the class sessions were similar to Nov 6 (SI Table S1). The peak
 403 concentration of 6-MHO and 4-OPA reached 0.56 ppb and 0.45 ppb, respectively, at
 404 ~11 am. Then concentrations rapidly decreased when occupancy was reduced to 21,
 405 consistent with the data measured in the previous week during similar occupancy
 406 variations. The agreement between model predictions (parameters extracted from Nov

407 6) and observed data for the concentrations of three compounds on Nov 13
408 demonstrates the effectiveness of the model with the fitted key parameters to simulate
409 the time-resolved changes in concentrations observed in the classroom. For a more
410 complete and quantitative comparison, Figure 5 provides scatter plots of all the model
411 predictions versus observations for ozone, 6-MHO and 4-OPA for the five test days at
412 the 3-min time resolution of the measured values. Correlations are strong with the
413 square of the correlation coefficient (R^2) in the range of 0.87-0.92, showing that the
414 model can explain approximately 90% of observed variability in the classroom with
415 excellent quantitative agreement (slopes show 1:1 lines). Besides, the analysis of model
416 prediction without surface interactions demonstrate that the R^2 of 6-MHO and 4-OPA
417 are reduced to 0.76 and 0.52, respectively. Thus, surface uptake can significantly
418 influence the accuracy of the model predictions.

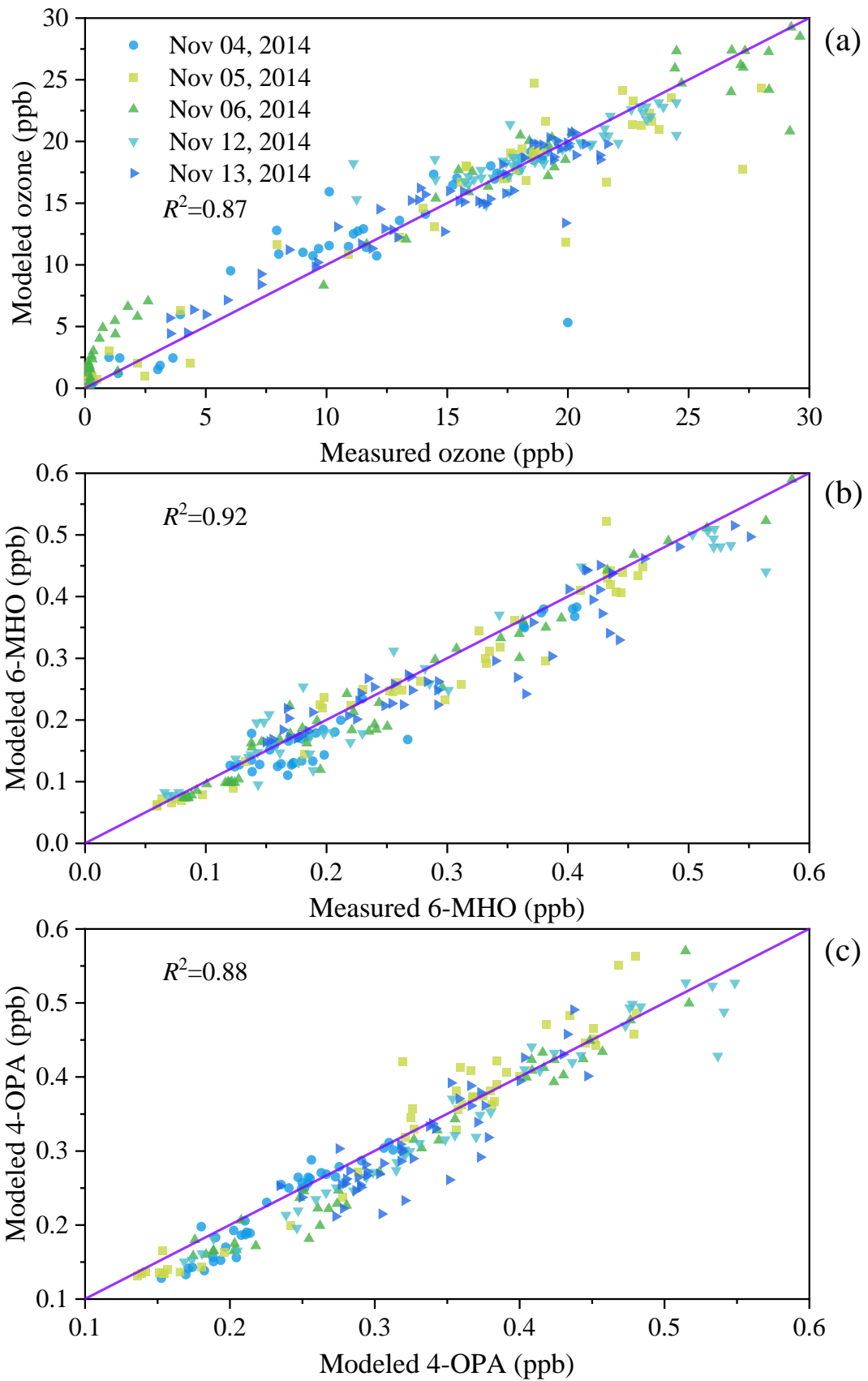
419 The above analysis focuses on modelling ozone/squalene dynamics in a classroom.
420 To check the feasibility of extending the developed model to other indoor settings, we
421 compare the model predictions with published data from experiments in a simulated
422 occupied office conducted by Wisthaler and Weschler²⁹. For the modelling, the reaction
423 rate constants of 6-MHO and 4-OPA are taken from the values obtained in this study
424 from classroom tests. Detailed information is included in SI Section S3 and Figure S6.
425 The good agreement between model prediction and experimental data in Figure S6
426 ($R^2=0.92-0.94$) demonstrates that the model can be applicable for predicting the
427 ozone/squalene dynamics in other indoor settings.



428

429 **Figure 4.** Comparison of model predictions with classroom observations for (a) ozone,

430 (b) 6-MHO, and (c) 4-OPA on Nov 13, 2014.



431

432 **Figure 5.** Correlation modeled results with measurements for (a) ozone, (b) 6-MHO,

433 and (c) 4-OPA.

434 **Limitations**

435 Although some real indoor environments (e.g., classroom, office) are investigated
436 in the presence of humans, there are limitations remaining in this study. For the present
437 study, we assume the squalene ozonolysis process occurs from the outer surface of
438 human skin, to simplify the interaction between ozone and occupants. In real reaction
439 processes, part of the human skin is bared to the ambient air, which can directly react
440 with ozone; part of the human skin is covered by clothing, the ozone may firstly
441 penetrate the clothing layer (barrier layer), then react with skin oil. So, the interaction
442 between human skin and ozone in real scenarios is very complicated, which deserves
443 further study to explore the relevance of squalene ozonolysis production and the kind
444 of clothing as well as skin coverage rate. In addition, the surface partition coefficients
445 should be different for different indoor material surfaces. In this study, to make the
446 model simple and practical, we assume all the surfaces have the same partition
447 coefficients, which is certainly not true for real scenarios. Detailed description for
448 different surface types is still needed to give a more accurate prediction with the model.
449

450 **Acknowledgments**

451 This study was supported by the Alfred P. Sloan Foundation (Grant No. 2016-7050),
452 and the National Natural Science Foundation of China (Grant No. 51778053, No.
453 51476013).

454

455 **Supporting Information**

456 Additional details on chemical reaction of ozone with squalene (Section S1), formation
457 rate of 6-MHO and 4-OPA (Section S2), application of model for other indoor settings
458 (Section S3); comparison of model prediction with observations for unoccupied period
459 (Figures S1), relative contribution of ozone removed by the various sinks (Figure S2),
460 comparison of model predictions with observations for Nov 4, Nov 5, and Nov 13
461 (Figure S3-S5), comparison of model prediction with measurements in literature in a
462 simulated office (Figure S6); occupants in the classroom during different class sessions
463 (Tables S1), parameters for modelling ozone/squalene reactions (Table S2), ozone
464 deposition velocity in different studies (Table S3). This material is available free of
465 charge via the Internet at <http://pubs.acs.org>.

466

467 **References**

- 468 (1) Streng, A. G. Tables of Ozone Properties. *J. Chem. Eng. Data* **1961**, *6* (3), 431-436.
- 469 (2) Gold, D. R.; Allen, G.; Damokosh, A.; Serrano, P.; Hayes, C.; Castiilejos, M.
470 Comparison of Outdoor and Classroom Ozone Exposures for School Children in
471 Mexico City. *J. Air Waste Manag. Assoc.* **1996**, *46* (4), 335-342.
- 472 (3) Barrese, E.; Gioffrè, A.; Scarpelli, M.; Turbante, D.; Trovato, R.; Iavicoli, S. Indoor
473 Pollution in Work Office: VOCs, Formaldehyde and Ozone by Printer. *Occup. Dis.*
474 *Environ. Med.* **2014**, *02* (03), 49-55.
- 475 (4) Britigan, N.; Alshawa, A.; Nizkorodov, S. A. Quantification of Ozone Levels in
476 Indoor Environments Generated by Ionization and Ozonolysis Air Purifiers. *J. Air*
477 *Waste Manag. Assoc.* **2006**, *56* (5), 601-610.

- 478 (5) Coleman, B. K.; Lunden, M. M.; Destailats, H.; Nazaroff, W. W. Secondary
479 organic aerosol from ozone-initiated reactions with terpene-rich household
480 products. *Atmos. Environ.* **2008**, *42* (35), 8234-8245.
- 481 (6) Singer, B. C.; Coleman, B. K.; Destailats, H.; Hodgson, A. T.; Lunden, M. M.;
482 Weschler, C. J.; Nazaroff, W. W. Indoor secondary pollutants from cleaning product
483 and air freshener use in the presence of ozone. *Atmos. Environ.* **2006**, *40* (35), 6696-
484 6710.
- 485 (7) Cheng, Y.-H.; Lin, C.-C.; Hsu, S.-C. Comparison of conventional and green
486 building materials in respect of VOC emissions and ozone impact on secondary
487 carbonyl emissions. *Build. Environ.* **2015**, *87*, 274-282.
- 488 (8) Gall, E.; Darling, E.; Siegel, J. A.; Morrison, G. C.; Corsi, R. L. Evaluation of three
489 common green building materials for ozone removal, and primary and secondary
490 emissions of aldehydes. *Atmos. Environ.* **2013**, *77*, 910-918.
- 491 (9) Hoang, C. P.; Kinney, K. A.; Corsi, R. L. Ozone removal by green building
492 materials. *Build. Environ.* **2009**, *44* (8), 1627-1633.
- 493 (10) Huang, Y.; Lee, S. C.; Ho, K. F.; Ho, S. S. H.; Cao, N. Y.; Cheng, Y.; Gao, Y. Effect
494 of ammonia on ozone-initiated formation of indoor secondary products with
495 emissions from cleaning products. *Atmos. Environ.* **2012**, *59*, 224-231.
- 496 (11) Tamás, G.; Weschler, C. J.; Bakó-Biró, Z.; Wyon, D. P.; Strøm-Tejsen, P. Factors
497 affecting ozone removal rates in a simulated aircraft cabin environment. *Atmos.*
498 *Environ.* **2006**, *40* (32), 6122-6133.
- 499 (12) Coleman, B. K.; Destailats, H.; Hodgson, A. T.; Nazaroff, W. W. Ozone

500 consumption and volatile byproduct formation from surface reactions with aircraft
501 cabin materials and clothing fabrics. *Atmos. Environ.* **2008**, *42* (4), 642-654.

502 (13) Pandrangi, L. S.; Morrison, G. C. Ozone interactions with human hair: Ozone
503 uptake rates and product formation. *Atmos. Environ.* **2008**, *42* (20), 5079-5089.

504 (14) Fadeyi, M. O.; Weschler, C. J.; Tham, K. W.; Wu, W. Y.; Sultan, Z. M. Impact of
505 human presence on secondary organic aerosols derived from ozone-initiated
506 chemistry in a simulated office environment. *Environ. Sci. Technol.* **2013**, *47* (8),
507 3933-3941.

508 (15) Fruekilde, P.; Hjorth, J.; Jensen, N. R.; Kotzias, D. Larsen, B. Ozonolysis at
509 vegetation surfaces: a source of acetone, 4-oxopentanal, 6-methyl-5-hepten-2-one,
510 and geranyl acetone in the troposphere. *Atmos. Environ.* **1998**, *32* (11), 1893–1902.

511 (16) Lakey, P. S. J.; Wisthaler, A.; Berkemeier, T.; Mikoviny, T.; Poschl, U.; Shiraiwa,
512 M. Chemical kinetics of multiphase reactions between ozone and human skin lipids:
513 Implications for indoor air quality and health effects. *Indoor Air* **2017**, *27* (4), 816-
514 828.

515 (17) Jarvis, J.; Seed, M.; Elton, R.; Sawyer, L.; Agius, R. Relationship between chemical
516 structure and the occupational asthma hazard of low molecular weight organic
517 compounds. *Occup. Environ. Med.* **2005**, *62* (4), 243-250.

518 (18) Anderson, S. E.; Wells, J. R.; Fedorowicz, A.; Butterworth, L. F.; Meade, B.;
519 Munson, A. E. Evaluation of the contact and respiratory sensitization potential of
520 volatile organic compounds generated by simulated indoor air chemistry. *Toxicol.*
521 *Sci.* **2007**, *97* (2), 355-363.

- 522 (19)Anderson, S. E.; Franko, J. F.; Jackon, L. G.; Wells, J. R.; Ham, J. E.; Meade, B. J.
523 Irritancy and allergic responses induced by exposure to the indoor air chemical 4-
524 oxopentanal. *Toxicol. Sci.* **2012**, *127* (2), 371-381.
- 525 (20)Wolkoff, P.; Larsen, S. T.; Hammer, M.; Kofoed-Sørensen, V.; Clausen, P. A.;
526 Nielsen, G. D. Human reference values for acute airway effects of five common
527 ozone-initiated terpene reaction products in indoor air. *Toxicol. Lett.* **2013**, *216*,
528 54-64.
- 529 (21)Petrick, L.; Dubowski, Y. Heterogeneous oxidation of squalene film by ozone
530 under various indoor conditions. *Indoor Air* **2009**, *19* (5), 381-391.
- 531 (22)Rai, A. C.; Guo, B.; Lin, C.-H.; Zhang, J. S.; Pei, J. J.; Chen, Q. Y. Ozone reaction
532 with clothing and its initiated particle generation in an environmental chamber.
533 *Atmos. Environ.* **2013**, *77*, 885-892.
- 534 (23)Duan, J. C.; Tan, J. H.; Yang, L.; Wu, S.; Hao, J. M. Concentration, sources and
535 ozone formation potential of volatile organic compounds (VOCs) during ozone
536 episode in Beijing. *Atmos. Res.* **2008**, *88* (1), 25-35.
- 537 (24)Wells, J. R.; Morrison, G. C.; Coleman, B. K. Kinetics and Reaction Products of
538 Ozone and Surface-Bound Squalene. *J. Astm Int.* **2008**, *5* (7), 1-12.
- 539 (25)Fu, D.; Leng, C. B.; Kelley, J.; Zeng, G.; Zhang, Y. H.; Liu, Y. ATR-IR study of
540 ozone initiated heterogeneous oxidation of squalene in an indoor environment.
541 *Environ. Sci. Technol.* **2013**, *47* (18), 10611-10618.
- 542 (26)Zhou, S. M.; Forbes, M. W.; Abbatt, J. P. D. Kinetics and Products from
543 Heterogeneous Oxidation of Squalene with Ozone. *Environ. Sci. Technol.* **2016**, *50*

- 544 (21), 11688-11697.
- 545 (27) Grosjean, E.; Grosjean, D.; Seinfeld, J. H. Gas-phase reaction of ozone with trans-
546 2-hexenal, trans-2-hexenyl acetate, ethylvinyl ketone, and 6-methyl-5-hepten-2-
547 one. *Int. J. Chem. Kinet.* **1996**, *28* (5), 373-382.
- 548 (28) Leonardo, T.; Silva, E. C. d.; Arbilla, G. Ozonolysis of Geraniol-trans, 6-Methyl-
549 5-hepten-2-one, and 6-Hydroxy-4-methyl-4-hexenal: Kinetics and Mechanisms. *J.*
550 *Phys. Chem. A* **2008**, *112* (29), 6636-6645.
- 551 (29) Wisthaler, A.; Weschler, C. J. Reactions of ozone with human skin lipids: sources
552 of carbonyls, dicarbonyls, and hydroxycarbonyls in indoor air. *Proc. Natl. Acad.*
553 *Sci. USA* **2010**, *107* (15), 6568-6575.
- 554 (30) Tang, X. C.; Misztal, P. K.; Nazaroff, W. W.; Goldstein, A. H. Siloxanes Are the
555 Most Abundant Volatile Organic Compound Emitted from Engineering Students in
556 a Classroom. *Environ. Sci. Technol. Lett.* **2015**, *2* (11), 303-307.
- 557 (31) Morrison, G. C.; Weschler, C. J.; Bekö , G. Dermal uptake directly from air under
558 transient conditions: advances in modeling and comparisons with experimental
559 results for human subjects. *Indoor Air* **2016**, *26* (6), 913-924.
- 560 (32) Yang, T; Xiong, J. Y.; Tang, X. C.; Misztal, P. K. Predicting indoor emissions of
561 cyclic volatile methylsiloxanes from the use of personal care products by university
562 students. *Environ. Sci. Technol.* **2018**, *52*, 14208-14215.
- 563 (33) Weschler, C. J.; Nazaroff, W. W. Semivolatile organic compounds in indoor
564 environments. *Atmos. Environ.* **2008**, *42* (40), 9018-9040.
- 565 (34) 6-Methyl-5-hepten-2-one Properties, 2019;
566 https://www.chemicalbook.com/ChemicalProductProperty_EN_CB4729000.htm

567 (accessed Jun 3, 2019)

568 (35) Weschler, C. J. Roles of the human occupant in indoor chemistry. *Indoor Air* **2016**,

569 26 (1), 6-24.

570 (36) Gao, K.; Xie, J. R.; Yang, X. D. Estimation of the contribution of human skin and

571 ozone reaction to volatile organic compounds (VOC) concentration in aircraft

572 cabins. *Build. Environ.* **2015**, 94, 12-20.

573 (37) Bhangar, S.; Huffman, J. A.; Nazaroff, W. W. Size-resolved fluorescent biological

574 aerosol particle concentrations and occupant emissions in a university classroom.

575 *Indoor Air* **2014**, 24 (6), 604-617.

576 (38) Tang, X. C.; Misztal, P. K.; Nazaroff, W. W.; Goldstein, A. H. Volatile Organic

577 Compound Emissions from Humans Indoors. *Environ. Sci. Technol.* **2016**, 50 (23),

578 12686-12694.

579 (39) Jordan, A.; Haidacher, S.; Hanel, G.; Hartungen, E.; Märk, L.; Seehauser, H.;

580 Schottkowsky, R.; Sulzer, P.; Märk, T. D. A high resolution and high sensitivity

581 proton-transfer-reaction time-of-flight mass spectrometer (PTR-TOF-MS). *Int. J.*

582 *Mass spectrom.* **2009**, 286, 122-128.

583 (40) Bois, D. D.; Bois, E. F. D. A formula to estimate the approximate surface area if

584 height and weight be known. *Nutrition* **1989**, 5 (5), 303-311.

585 (41) Huang, H. Y.; Haghghat, F. Modelling of volatile organic compounds emission

586 from dry building materials. *Build. Environ.* **2002**, 37 (12), 1349-1360.

587 (42) Yang, X. D.; Chen, Q.; Zhang, J. S.; Magee, R.; Zeng, J.; Shaw, C. Y. Numerical

588 simulation of VOC emissions from dry materials. *Build. Environ.* **2001**, 36 (10),

589 1099-1107.

590 (43) Xiong, J. Y.; Yao, Y.; Zhang, Y. P. C-history method: rapid measurement of the
591 initial emittable concentration, diffusion and partition coefficients for
592 formaldehyde and VOCs in building materials. *Environ. Sci. Technol.* **2011**, *45* (8),
593 3584-3590.

594 (44) Weschler, C. J. Ozone in indoor environments: concentration and chemistry. *Indoor*
595 *Air* **2000**, *10* (4), 269-288.

596 (45) Morawska, L.; He, C.; Johnson, G.; Guo, H.; Uhde, E.; Ayoko, G. Ultrafine
597 Particles in Indoor Air of a School: Possible Role of Secondary Organic Aerosols.
598 *Environ. Sci. Technol.* **2009**, *43* (24), 9103-9109.

599 (46) EPA. Exposure Factors Handbook. National Center for Environmental Assessment,
600 Washington, DC, **1997**.

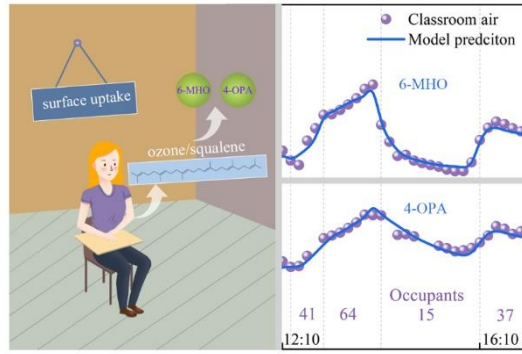
601 (47) Rim, D.; Gall, E. T.; Ananth, S.; Won, Y. Ozone reaction with human surfaces:
602 Influences of surface reaction probability and indoor air flow condition. *Build.*
603 *Environ.* **2018**, *130*, 40-48.

604 (48) Singer, B. C.; Hodgson, A. T.; Hotchi, T.; Ming, K. Y.; Sextro, R. G.; Wood, E. E.;
605 Brown, N. J. Sorption of organic gases in residential rooms. *Atmos. Environ.* **2007**,
606 *41* (15), 3251-3265.

607

608

TOC Art



609